EFFECT OF IN-PLANE FIBRE WAVINESS IN CONTINUOUS TOW SHEARING ON LAMINATE PROPERTIES

Charles P. Macleod[1*], Alex Prado[2], Pedro H. Cabral[2], Jonathan Cooper[1], Byung Chul Kim[1*]

[1] Bristol Composites Institute (BCI), Queen's Building, University Walk, Bristol, BS8 1TR, UK
[2]Technology Development, Embraer S. A., São José dos Campos, Brazil
Corresponding authors *(charles.macleod@bristol.ac.uk and B.C.Eric.Kim@bristol.ac.uk)

Keywords: Automated fibre placement (AFP), Continuous tow shearing (CTS), Process-induced defects, Non-destructive testing (NDT)

ABSTRACT

Continuous Tow Shearing (CTS) is a novel automated fibre placement process that enables fibre-steering using wide unidirectional prepreg tapes without tape buckling. However, when the CTS process steers the fibres utilising the in-plane shear deformation of the tape, the inherently misaligned fibres within the tape buckle generating fibre waviness. This behaviour may pose a new challenge in assessing the fibre waviness in a large area and predicting its impact on mechanical properties.

In this work, a large-area optical scaning method in conjunction with a Structure Tensor based image Analysis (STA), which is often used in cellular biology to analyse fibrillar structures, was applied, and its feasibility to quantitatively assess the fibre waviness in a non-destructive way was investigated. First, the STA process parameters were calibrated by comparing microscopic STA with a conventional method. Then, STA was used to investigate the relationship between the shear angle and the fibre waviness level within CTS fibre-steered lay-ups. This process was followed by finding correlations between the fibre waviness and the mechanical properties of the cured laminates obtained experimentally. The results showed that STA is a fast and cost-effective way to analyse the quality of CTS produced fibre-steered laminates with potential for in-line quality inspection.

1. INTRODUCTION

Developed in response to the shortcomings of Automated Fibre Placement (AFP), Continuous Tow Shearing (CTS) utilises the in-plane shear deformation of carbon fibre tapes to produce high-quality, fibre-steered laminates with minimal defects when compared to similar fibre-steered AFP laminates [1,2]. However, due to the inherently stochastic distribution of fibre alignments within the tape material [3], not all fibres can be perfectly aligned and thus some in-plane fibre waviness is generated during shearing. The magnitude and severity of in-plane fibre waviness increases with the shear angle of the tape due to micro-scale in-plane buckling of the fibres with excess lengths during shearing. The exact influence that this waviness has on the mechanical properties of CTS-produced laminates has not been investigated yet.

The quantitative assessment of fibre waviness is as challenging as its detection. In the past, light intensity scanning algorithms [4] and Fourier transform algorithms [5] have been used, with the latest method being a binarised image analysis algorithm called High Resolution Misalignment Analysis (HRMA) [6,7]. However, the key limitation with these methods is that they work for micrographs taken from samples in destructive ways. Shear-induced fibre waviness in CTS fibre-steering can vary along the steered path, thus fibre waviness is not a localised feature but a global feature, so a new fast and non-destructive approach that can measure fibre waviness on a macroscopic scale is needed.

This work proposes a unique image analysis approach based on structure tensors for measuring fibre waviness in high-resolution image scans taken from the tape surface. The proposed method, Structure Tensor Analysis (STA), is popular in the bio-medical field for measuring the alignment and waviness of microscopic collagen fibres. In this work, the STA method was calibrated against the current state-of-the-art HRMA method, and was applied to image scans, taken before and after curing, of the tensile specimens prior to testing. The tensile properties of the CTS produced laminates were subsequently correlated to the fibre waviness levels measured by STA.

2. IMAGE ANALYSIS METHODOLOGY

2.1. Structure Tensor Analysis (STA)

Structure Tensor Analysis (STA) relies on image gradients to calculate the structure tensor; more information on the mathematics of the STA method have been elaborated in [8]. The structure tensor is a localised covariance matrix that shows how the greyscale intensities vary in an image with respect to changes in the x and y positions within a Gaussian local window. Since image gradients are sensitive to noise, the image is smoothed by first applying a Gaussian blur [8]. The convolution and gradient operators are associative and commutative, thus the image's gradient can be calculated directly by convolving the image with the gradient of the Gaussian distribution [9]. This is done by creating a local window that is equal in size to four standard deviations of the Gaussian distribution (σ) away from the centre pixel. The local window is convolved with an identically sized Gaussian kernel which is a matrix composed of the discretised and normalised values of the gradient of the Gaussian distribution. The result is the gradient of the Gaussian blurred image which is used to calculate the structure tensor. The significance of the structure tensor is that it contains information on the dominant orientation of the local window as well as the coherency in its alignment. The local predominant orientation, θ, in the local window is the direction given by the largest eigenvector. The maximum absolute value of all θ measurements is θ_{max} which is used to relate the fibre waviness level to the laminate's mechanical properties. The STA method is available as a plug-in called OrientationJ [10] for the open-source image analysis tool ImageJ/FIJI.

2.2. Calibration

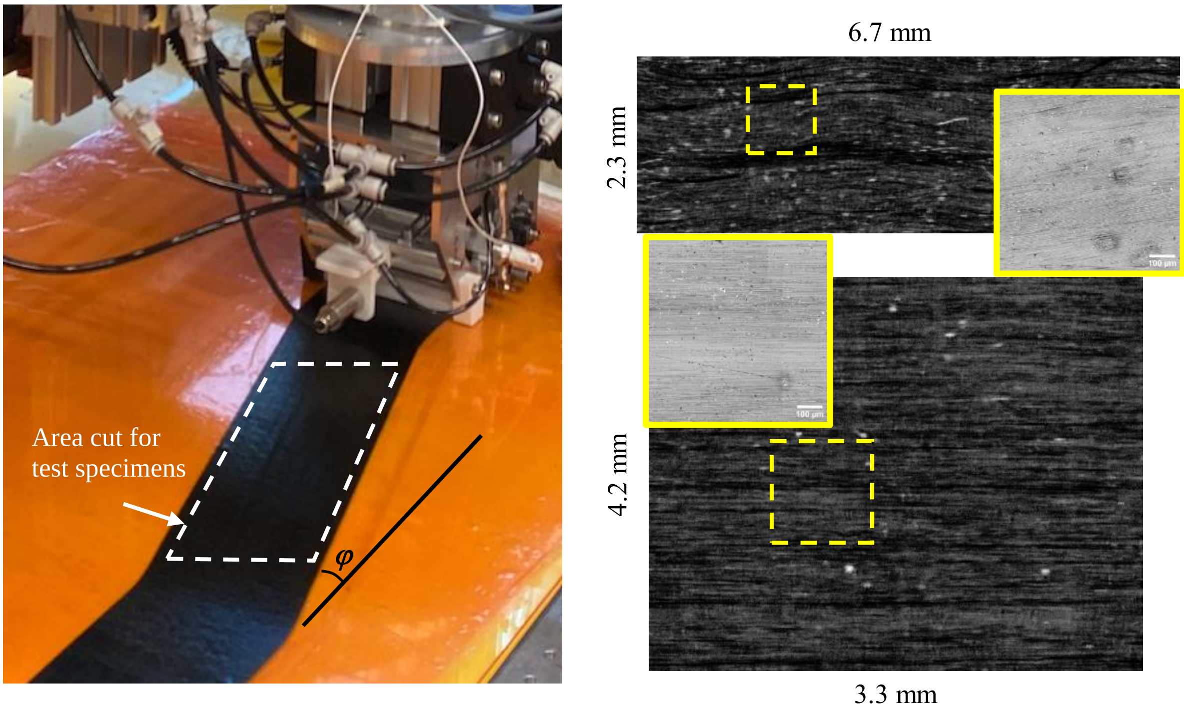

Figure 1: (Left) Constant shear angle layup using a CTS prototype machine; (Right) Scanned sub-ROI for 45° (top) and 0° (bottom) and microscopic inset regions in yellow.

Pixel resolution (µm/px)	0.27
Detectable fibre diameter (µm)	2.00
Minimum fibre diameter (µm)	0.8
Cell size (µm)	20
Minimum aspect ratio between fibre length and diameter	3

Table 1: HRMA parameters

Local window size (pixels)	6
Cell size (µm)	300 µm
Gradient sampling method	Gaussian derivative method
Resolution (dpi)	1200 dpi to 4800 dpi
θ_{max} calculation method	1.5 interquartile range method

Table 2: Calibrated STA parameters

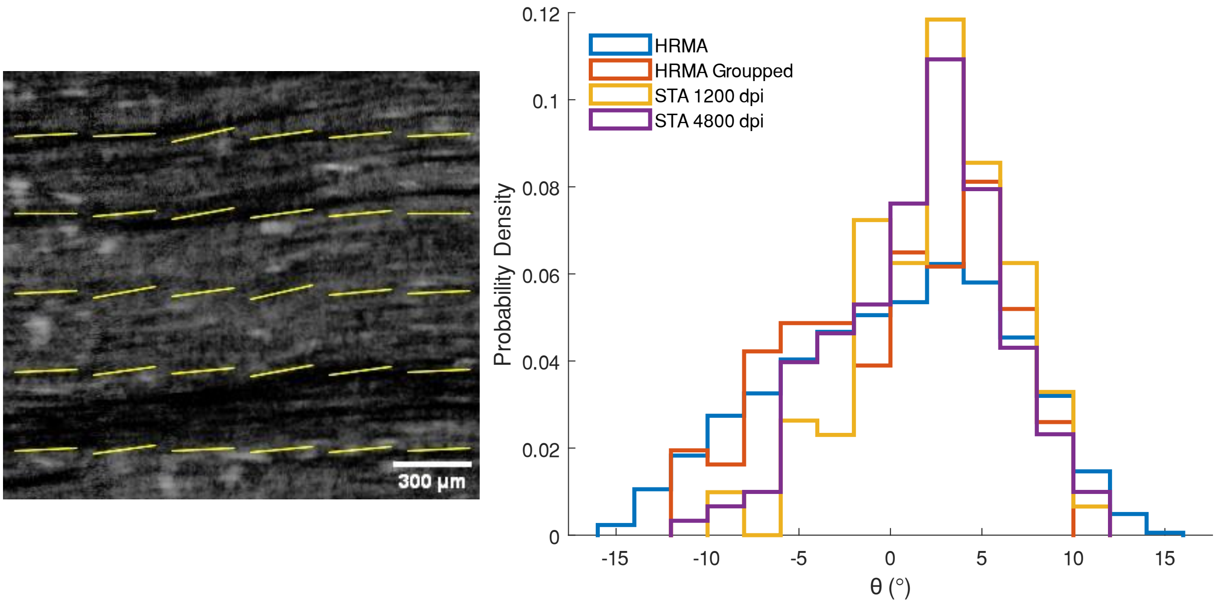

Figure 2: (Left) Scanned surface of the 45° sub-ROI from a CTS-steered laminate surface (yellow lines show the local fibre angles calculated by the STA); (Right) the fibre misalignment distribution for the 45° sub-ROI for 1200 dpi and 4800 dpi case.

The image processing parameters used in the STA method were calibrated by selecting those that returned a result closest to those of the HRMA method's microscopic measurements. Two CTS produced cured laminates were imaged; one was unsheared and the other was sheared at a constant angle of 45° as these specimens embodied the two extremes of fibre waviness levels. The CTS production methods are described later in Section 3.1. A region of interest (ROI) of approximately 20 mm × 20 mm was marked on the surface of the samples and was imaged using a microscope (Axio Imager M2, Zeiss, DE) at 200× magnification and with a resolution of 3.704 px/µm. It should be noted that micrographs were captured without polishing the surface by automatically controlling the depth of focus within the microscope's software. The micrographs were stitched using the Microscopy Image Stitching Tool (National Institute of Standards and Technology, US) in FIJI.

Scans of the same ROI were captured using a Contact Image Sensor (CIS) scanner (Perfection V39 scanner, Epson, JP) at the scanner's maximum resolution of 4800 dpi (0.189 px/µm) and then scaled down to 1200 dpi (0.047 px/µm) in increments of 400 dpi to check the effect of scanning resolution. For efficiency of the image processing, sub-ROIs were selected for analysis as shown in Figure 1. The size of the sub-ROI for the 0° and 45° specimens were 4.2 mm × 3.3 mm and 6.7 mm × 2.3 mm, respectively. Due to the circular cross-section of the carbon fibres, the light absorptivity of the fibre/matrix system is dependent on the light's polarisation [11]; the absorptivity is minimised when the light is polarised parallel to the fibre direction, thus the scanning direction was oriented transverse to the fibres, i.e. the integrated LED light bar was oriented parallel to the fibre direction.

The micrographs were analysed via HRMA with the parameters shown in Table 1, whilst the scanned images were analysed via STA and the calibrated parameters are shown in Table 2. Note that HRMA is sensitive to the input fibre diameter, and since the samples were unpolished, the visible section of the fibres was limited to above their midplane. Thus, a detectable fibre diameter of 2 μm was measured from the micrographs and used as the input for the HRMA.

Due to image noise, outlier measurements exist and can skew the θ_{max} value. Wilhelmsson et al. [7] calculated the 99th percentile value of all fibre misalignment angles and used it as θ_{max}, and removed values beyond θ_{max}. The HRMA method in this work uses the same approach, whilst the 1.5 interquartile range method provided by MATLAB's built-in 'rmoutliers' function [12], which was found to be more accurate at processing the STA results and was used to calculate the STA's θ_{max}.

Figure 2 shows a portion of the scanned surface of the 45° sub-ROI and its fibre misalignment angle distribution from the HRMA and STA methods. It was found that the scanning resolution did not significantly affect the results above 1200 dpi (0.047 px/μm). However, the 45° sub-ROI has a different microscopic orientation distribution than its corresponding scan orientation distribution. Individual fibres within a wavy tow have their own orientation distribution, and whilst their mean value equals the orientation of the tow, the θ_{max} is strongly affected by the extreme orientation of individual fibres. Thus, HRMA measured a greater θ_{max} value of 14.8° and a higher standard deviation of 6.2° compared to 10.8° and 4.1° for the STA method. This discrepancy was accounted for by groupping the individual HRMA measurements into 300 μm cells (the same cell size used for STA), which led to the θ_{max} and standard deviation of 11.8° and 5.4°, respectively. By comparison, the 0° sub-ROI does not have this difference in distributions because there are no wavy tows to affect the alignment and distribution of the fibres, therefore the θ_{max} and standard deviation from the HRMA (4.4º and 1.3º) were very close to those from the STA measured 3.4° and 1.3°, respectively.

3. EXPERIMENTAL METHODOLOGY

3.1. Specimen manufacture

As shown in Figure 1, unidirectional (UD) carbon fibre/epoxy prepreg tapes (IM7/8552 (12K)-134-33%, Hexcel, US) with a width of 100 mm were sheared at a constant shear angle using the University of Bristol's prototype CTS machine. The selected shear angles were from 0º to 45º, at a constant speed of 5 mm/s, a processing temperature of approximately 80°C. The shear-induced fibre waviness is dependent on process parameters such as tape temperature and tension as well as the inherent fibre misalignment within the tape material [13]. In the present study, the fibre direction tension applied to the prepreg tape was maintained to approximately 0.8 N/mm, which was not to minimise the waviness but to deliberately introduce waviness.

Multiple tapes were laid along the same path and then the sheared section was cut into a rectangular shape. As a result of the shear-induced tape thickness change, the cured ply thickness increases as a function of shearing angle ($t = t_0/\cos(\varphi)$), where t_0 is the unsheared CPT (0.125 mm) and φ is the shearing angle [2]. To maintain a constant laminate thickness of approximately 1 mm for tensile tests, the number of plies was reduced at greater shearing angles. After the plies were laid up, the sheared plies were cut and stacked, and then were cured in an autoclave following the curing cycle recommended by the material supplier (2 hours at 180ºC and at 7 bar). Caul plates were used to ensure a uniform specimen thickness and a good surface finish. Tensile test specimens were cut from the cured laminates using a CNC precision diamond wheel cutter and tapered fibreglass end tabs were bonded using epoxy adhesive (Araldite 2011, Huntsman, US).

3.2. Sample imaging and waviness analysis

For fibre waviness analysis of the tensile test specimens, the sheared section of each laid tape was scanned at a minimum resolution of 1600 dpi. Also, the surface of the cured laminates was subsequently rescanned to check any changes in fibre waviness after curing. The fibre waviness of each specimen was analysed using the calibrated STA method described in Sections 2.1-2.2 and the maximum misalignment angle, θ_{max}, was obtained.

3.3. Tensile testing method

The tensile tests were carried out following ASTM D3039 [14]. The calibrated STA's θ_{max} values were correlated to mechanical testing data to investigate any mechanical property knock-down factor related to in-plane fibre waviness. Specimen dimensions were 250 mm × 15 mm × ≈1 mm, these dimensions were checked prior to testing by measuring the specimens with a micrometer. They were tested using a universal testing machine with a 100 kN load cell (Instron 8801, Instron, US) at a constant crosshead speed of 2 mm/min. Strain was measured with a video extensometer (MG146B PoE, iMETRUM, UK). Table 3 shows details on the number of specimens tested.

Shearing angle (°)	Number of panels	Total number of specimens	Plies per panel	Thickness (mm)
0	2	8	8	1.0
15	2	10	8	1.0
30	3	12	7	1.0
45	4	12	6	1.1

Table 3: Tensile testing matrix

4. RESULTS

4.1. Tensile testing results

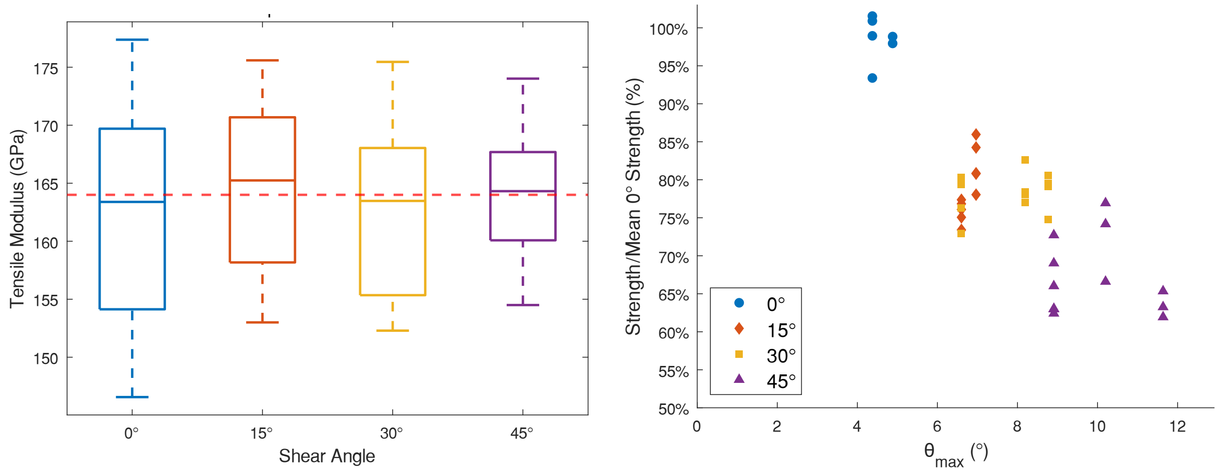

Figure 3: (Left) Tensile moduli for the specimens with different shearing angles, material spec. 164 GPa shown as a red dashed line; (Right) Tensile strengths vs. θ_{max}, note that θ_{max} is measured on a panel level and the value is compared to strengths which were measured on a specimen level.

As shown in Figure 3, the tensile modulus for all the specimens fell within a statistically similar range of an average of 163.6±7.4 GPa, which is the same as that in the material datasheet of 164 GPa. The average ultimate tensile strengths for the 0°, 15°, 30°, and 45° samples were 2843.3 ±100.9 MPa, 2240.0 ± 113.0 MPa, 2225.3 ± 78.0MPa, and 1911.5 ± 144.7 MPa, respectively. Prior to testing, the uncured and cured panels were analysed via the calibrated STA method, described previously. The difference between the uncured and cured θ_{max} values was marginal at 0.64°. Thus, to have more data points the data from both the uncured and cured scans was used to calculate the average θ_{max} of each panel. It is important to note that the image analysis was carried out on a panel level rather than a specimen level, hence specimens from the same panel have the same θ_{max} value. The specimens failed with transverse splitting as well as localised fibre failure.

5. DISCUSSION

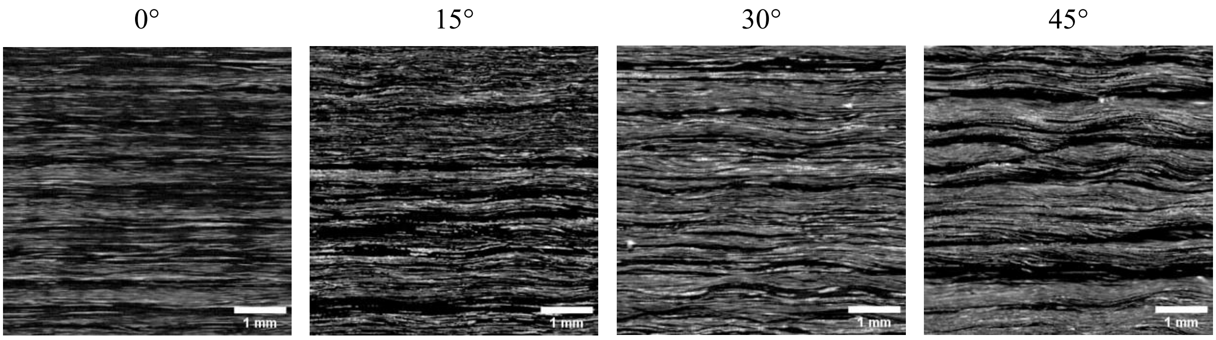

Figure 4: Close up view of fibre waviness within the tensile specimens, as captured by surface scans.

As shown in Figure 4, fibre waviness is not uniformly distributed throughout the specimen, and because of the initial stochastically varying fibre alignments, wavy fibres are mixed with straightened fibres. Fibres that are aligned positively to the shearing direction must be straightened, whilst those aligned negatively to the shearing direction would buckle and become wavy. Therefore, to reduce the severity of fibre waviness that would occur, fibre tension should increase as the shear angle increases, which was shown in the previous material level shear tests [13]. Furthermore, if the inherent fibre misalignment within the material is too high, tensioned fibres might not be able to be straightened even with an increase in the fibre tension level. Both material and processing conditions are important.

With the fibre tension, which was not ideally set for the purpose of this study, it was clearly demonstrated that in-plane shear-induced fibre waviness can significantly decrease the laminate's tensile strength in the CTS process. As shown in Figure 3 and Figure 4, the level of fibre waviness increased with shearing angle and correspondingly the laminate's tensile strength decreased. There is a correlation between the fibre waviness level (θ_{max}) and the tensile strength, and the proposed STA method was demonstrated to be an effective method to quantitatively assess the fibre waviness level.

6. CONCLUSION

Shear-induced fibre waviness can be a by-product of the CTS process when the inherent fibre misalignment level within the unidirectional tape is high or the process parameters such as fibre tension and temperature are not chosen based on a proper material characterisation test. In this paper, fibre waviness was shown to negatively affect tensile strength whilst having no impact on the tensile modulus. Therefore, a method of analysing fibre waviness in a macroscopic level is crucial to certify the CTS processing conditions as well as the suitability of the material used.

In this paper, a proposed STA method was demonstrated to accurately detect the fibres and was able to measure their local orientation without the need for detailed micrographs. The STA method requires careful consideration of the θ_{max} calculation method as it will greatly impact the accuracy of STA if outliers are not properly removed. Compared to the microscopic HRMA method and other similar microscopic approaches, the macroscopic application of STA has the advantage of being able to globally analyse a large surface, and this method has potential as a non-destructive evaluation tool for quality-inspection of laminates produced by the CTS process or other similar processes such as AFP.

ACKNOWLEDGEMENTS

This research was supported by the Industrial and International Leverage Fund (IILF) as part of the Engineering and Physical Sciences Research Council (EPSRC) Doctoral Training Partnership (DTP) and Embraer S. A.. The authors would also like to thank Dr. Bohao Zhang for his assistance with preparing the micrographs and the tensile specimens.

REFERENCES

[1] B.C. Kim, K. Potter, P.M. Weaver, Continuous tow shearing for manufacturing variable angle tow composites, *Composites Part A: Applied Science and Manufacturing*, **43**, 2012, pp. 1347–1356 (doi: 10.1016/j.compositesa.2012.02.024).

[2] B.C. Kim, P.M. Weaver, K. Potter, Manufacturing characteristics of the continuous tow shearing method for manufacturing of variable angle tow composites, *Composites Part A: Applied Science and Manufacturing*, **61**, 2014, pp. 141–151 (doi: 10.1016/j.compositesa.2014.02.019).

[3] K. Potter, C. Langer, B. Hodgkiss, S. Lamb, Sources of variability in uncured aerospace grade unidirectional carbon fibre epoxy preimpregnate, *Composites Part A: Applied Science and Manufacturing*, **38**, 2007, pp. 905–916 (doi: 10.1016/j.compositesa.2006.07.010).

[4] C. Creighton, M.P.F. Sutcliffe, T.W. Clyne, A multiple field image analysis procedure for characterisation of fibre alignment in composites, *Composites Part A: Applied Science and Manufacturing*, **32**, 2001, pp. 221–229 (doi: 10.1016/S1359-835X(00)00115-9).

[5] K.K. Kratmann, M.P. Sutcliffe, L.T. Lilleheden, R. Pyrz, O.T. Thomsen, A novel image analysis procedure for measuring fibre misalignment in unidirectional fibre composites, *Composites Science and Technology*, **69**, 2009, pp. 228–238 (doi: 10.1016/j.compscitech.2008.10.020).

[6] D. Wilhelmsson, L.E. Asp, A high resolution method for characterisation of fibre misalignment angles in composites, *Composites Science and Technology*, **165**, 2018, pp. 214–221 (doi: 10.1016/j.compscitech.2018.07.002).

[7] D. Wilhelmsson, R. Gutkin, F. Edgren, L.E. Asp, An experimental study of fibre waviness and its effects on compressive properties of unidirectional NCF composites, *Composites Part A: Applied Science and Manufacturing*, **107**, 2018, pp. 665–674 (doi: 10.1016/j.compositesa.2018.02.013).

[8] Z. Püspöki, M. Storath, D. Sage, M. Unser, *Transforms and Operators for Directional Bioimage Analysis: A Survey*, Advances in Anatomy, Embryology, and Cell Biology, Vol. 219, 2016, pp. 69–93 (doi: 10.1007/978-3-319-28549-8_3).

[9] P. Mlsna, J. Rodriguez, *Gradient and Laplacian Edge Detection*, Handbook of Image and Video Processing, 2nd ed., Elsevier, 2005(doi: 10.1016/B978-0-12-119792-6.X5062-1).

[10] D. Sage, OrientationJ, 2020,. http://bigwww.epfl.ch/demo/orientation/#soft.

[11] C. Freitag, R. Weber, T. Graf, Polarization dependence of laser interaction with carbon fibers and CFRP, *Optics Express*, **22**, 2014, pp. 1474 (doi: 10.1364/OE.22.001474).

[12] rmoutliers Detect and remove outliers in data, *MathWorks*, 2018,. https://uk.mathworks.com/help/matlab/ref/rmoutliers.html#mw_f334bff5-af8a-45f3-a025-2d4bb1909464 (accessed January 26, 2023).

[13] B. Zhang, B.C. Kim, Experimental characterisation of large in-plane shear behaviour of unidirectional carbon fibre/epoxy prepreg tapes for continuous tow shearing (CTS) process, *Composites Part A: Applied Science and Manufacturing*, **162**, 2022, pp. 107–168 (doi: 10.1016/j.compositesa.2022.107168).

[14] ASTM, Astm D3039/D3039M - 17 Standard Test Method for Tensile Properties for Polymer Matrix Composite Materials, *Annual Book of ASTM Standards*, 2017, pp. 1–13 (doi: 10.1520/D3039_D3039M-17).